Measuring the EUV-induced contamination rates of TiO_2-capped multilayer optics by anticipated production-environment hydrocarbons

S. B. Hill[*] [a], N. S. Faradzhev[b], C. S. Tarrio[a], and T. B. Lucatorto[a], R. A. Bartynski[b],
B. V. Yakshinskiy[b], and T. E. Madey[b]
[a] National Institute of Standards and Technology, Gaithersburg, MD 20899 USA
[b] Dept. of Physics and Astronomy, and Laboratory for Surface Modification,
Rutgers, The State University of New Jersey, Piscataway NJ 08854 USA

ABSTRACT

The primary, publicly reported cause of optic degradation in pre-production extreme-ultraviolet (EUV) lithography systems is carbon deposition. This results when volatile organics adsorb onto optic surfaces and then are cracked by EUV-induced reactions. Hence the deposition rate depends on the adsorption-desorption kinetics of the molecule-surface system as well as the basic photon-stimulated reaction rates, both of which may vary significantly for different organic species. The goal of our ongoing optics-contamination program is to estimate the contamination rate of species expected in the tool environment by exposing samples to in-band 13.5 nm light from our synchrotron in the presence of fixed partial pressures of admitted gases. Here we report preliminary results of contamination rates on TiO_2-capped samples for species observed in resist-outgassing measurements (benzene, isobutene, toluene and tert-butylbenzene) in the pressure range (10^{-6} to 10^{-4}) Pa which all display an unexpected logarithmic dependence on pressure. This scaling is in agreement with previous EUV exposures of other species at NIST as well as independent measurements of coverage performed at Rutgers University. These results are consistent with a molecular desorption energy that decreases with coverage due to molecular interactions (Temkin model). Use of the proper scaling law is critical when estimating optic lifetimes by extrapolating over the 3-to-6 orders of magnitude between accelerated-testing and tool-environment partial pressures.

Keywords: Extreme ultraviolet lithography (EUVL); EUV optics contamination; TiO_2; EUV optics lifetime; carbon deposition; carbon contamination

1. INTRODUCTION

The commercialization of extreme-ultraviolet (EUV) lithography high-volume manufacturing will require the multilayer mirrors (MLMs) in the projection-optics box of a stepper to have a lifetime of 30 000 h without a decrease in reflectivity of more than a few percent.[1,2] Recent experience in several laboratories with pre-production EUV steppers has shown that carbonization is the major source of reflectivity loss, and that loss of over a few percent on some optics occurs after only a small fraction of the required lifetime. The carbonization is caused by the photon-induced cracking of organic contaminants adsorbed onto the optic surface from the ambient vacuum of the stepper originating from resist outgassing and the components of the vacuum environment in the tool. The National Institute for Standards and Technology (NIST), in collaboration with Rutgers University, has an ongoing program to measure and understand the carbon growth processes well enough to make reasonable estimates of the lifetime and contamination rates to be expected in the high-volume manufacturing environment of an EUV lithography tool. Since most testing at NIST and elsewhere is performed at partial pressures several orders of magnitude higher than actual tool conditions, predicting behavior under actual conditions requires an understanding of how carbonization rates scale with partial pressure and how the relatively high levels of water vapor in the stepper can affect the process.

[*] shannon.hill@nist.gov; phone (301) 975 4283; fax (301) 926 2746

2. MEASUREMENT OF CONTAMINATION RATES

2.1 NIST EUV exposure facility

The end station installed at the Synchrotron Ultraviolet Radiation Facility (SURF-III) and illustrated in Fig. 1 was designed to maximize throughput and minimize vacuum contamination associated with sample introduction. The vacuum chamber has a well controlled vacuum environment achieved in part by a smooth electropolished finishing. Most of the components exposed to vacuum are plated with a ≈0.5 µm layer of gold to minimize adsorption of water and contaminant species on the chamber walls. The exposure chamber is bakeable to 150º C, limited only by the photodiodes used to measure the intensity of the incident and reflected EUV radiation. Samples are introduced through a gold-plated load lock. All pumps are completely oil free. The base pressure in the chamber is routinely in the low-10^{-8} Pa range. Analysis with a quadrupole mass spectrometer (QMS) reveals no peaks greater than 10^{-10} Pa above a mass-to-charge ratio of 44 u/e out to the measurement limit of 200 u/e.

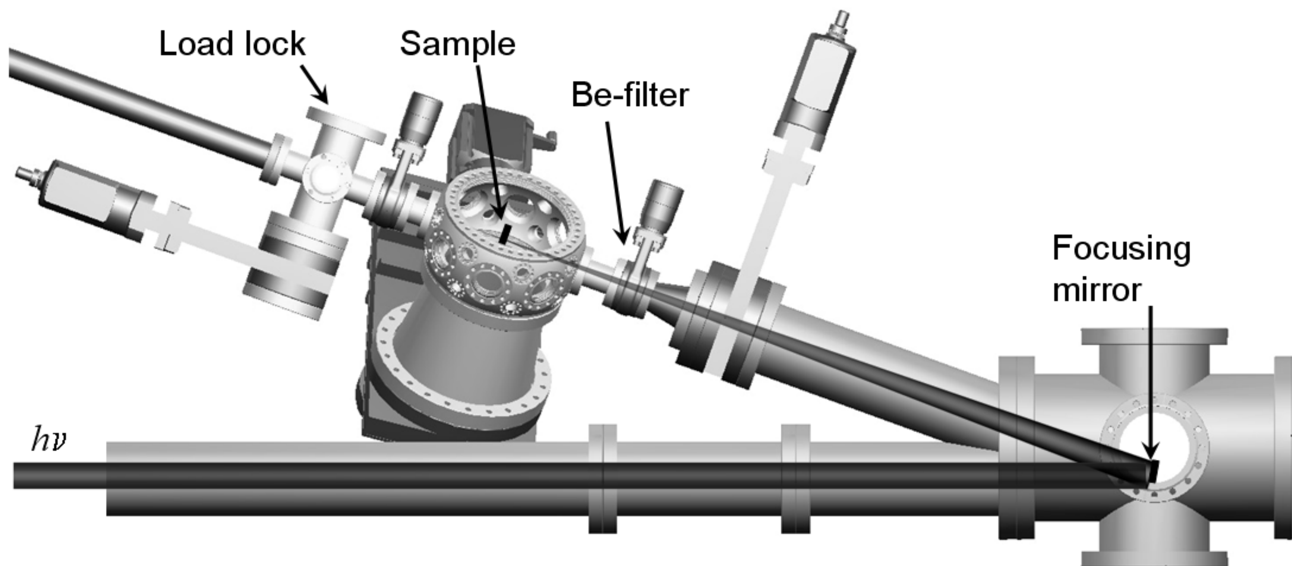

Figure 1. Schematic of the end-station on the SURF III synchrotron for EUV-optics contamination testing at NIST.

The output of the synchrotron is collected by a near-normal-incidence MLM optic placed approximately 4 m from the storage ring tangent point. This MLM is designed to reflect EUV radiation with a 6-degree angle of incidence in the bandwidth 13.1 nm to 13.6 nm with approximately 50 % efficiency. Due to pre-existing geometry, however, the angle of incidence is 10°. A 200-nm-thick beryllium filter completely blocks long-wavelength light while transmitting 50 % to 60 % of the EUV radiation. More importantly, this filter also serves as a physical barrier separating the exposure chamber from the rest of the beamline. It is essential that the synchrotron and the focusing mirror not be exposed to the high levels of water and/or organic vapors present in the exposure chamber. The power of the exposure beam on the sample is checked periodically by a calibrated photodiode.

The MLM under test is placed near the focal spot of the EUV beam and oriented to reflect the incident radiation at 9º. The focal spot has an asymmetric, approximately Gaussian intensity distribution with full-widths at half maxima of 1.0 mm and 0.7 mm. The peak intensity at the center of the spot follows the synchrotron decay cycle and decreases smoothly over the range (8 to 4) mW/mm^2 over the course of approximately 8 h before a new beam is injected. A single beam-decay cycle will provide an integrated EUV dose of approximately 120 J/mm^2 at center of the exposure spot. Typical peak doses for our exposures range from 40 to 160 J/mm^2.

The contamination precursors (benzene, toluene, water, etc) are admitted to the vacuum chamber from two separate gas manifolds through individual high-precision, all-metal leak valves. Partial pressures of admitted hydrocarbons are measured with a Bayard-Alpert ionization gauge with an absolute uncertainty of 20% and, unless stated otherwise, are reported here after correction for the sensitivity factors for each gas.[3] Prior to use, all gasses are subjected to multiple

freeze-pump-thaw cycles to remove primarily water and air impurities. Gas purity was then checked with QMS. During EUV exposures both QMS and ion gauge filaments remained off to avoid excessive heating of the sample and production of reactive species on the surface of the hot filaments.

2.2 EUV exposures: samples and conditions

Much of the initial work performed in this laboratory and elsewhere has studied contamination by exposing EUV mirror samples comprised of a full multilayer stack of 50-70 Mo:Si bilayers with various capping layers (e.g., Si, Ru, TiO_2). We have found strong evidence that the measured contamination rates can be significantly influenced by slight changes in the resonance conditions when the MLMs are irradiated with resonant 13.5 nm EUV light.[4] It is not surprising that the contamination rate should depend on the position of the optic surface within the standing wave created by resonant irradiation of the MLM. If the optic surface is near a node, then the local density of photons will be much smaller than if the surface were near a maximum of intensity. Although it is strongly suspected that the cracking of the adsorbed carbonaceous molecules is caused by low-energy secondary electrons rather than direct photon processes,[5,6] similar resonance behavior is expected for photoemission since only those low-energy secondary electrons created within a few nanometers of the surface escape due to the very short, (1-2) nm, mean-free path of low-energy electrons. Indeed, direct secondary-electron yield (SEY) measurements of specially designed ML samples have shown pronounced variation between samples designed with surfaces near maxima and minima of the resonant standing wave. [7] So regardless of whether the contamination process is caused by the primary photons or the secondary electrons, the growth rate on two differently designed MLMs with identical capping layers could be quite different. Furthermore, if exposures are performed that deposit several nanometers of C, the contamination rate would vary with dose as the C layer grows through the intensity standing wave.

Since our goal is to characterize the contamination process for different contaminant species on various capping surfaces rather than to simply measure the contamination rate for a specific MLM design and dose, we have chosen to avoid confounding the resonance effects described above with the contamination processes by using non-resonant tri-layer samples that consist of only the top Mo and Si layers of a typical ML stack with an amorphous 1.5-nm-thick TiO_2 capping layer.[8] This configuration was chosen to have a photoelectron yield and energy distribution similar to a full MLM when exposed to resonant 13.5 nm light. Use of non-reflective samples precludes analysis with reflectometry, but as will be discussed below, using the reflectivity change of a MLM to determine C thickness is just as susceptible to confounding by resonance effects as is the contamination process itself. Of course the resonance effects could also be avoided by exposing standard MLMs to broadband or non-resonant light; however, there is some evidence that the damage rates may vary with wavelength,[9] as one might expect since the attenuation lengths for the relevant materials (Mo, SiO_2, TiO_2, Ru) vary significantly over the range (10-40) nm.[10]

Studies at Rutgers of carbon deposition from electron-beam irradiation of TiO_2(011) surfaces in the presence of benzene or methyl methacrylate (MMA) have demonstrated that the growth rate slows after deposition of a certain initial thickness.[11] This may be interpreted as a change in the contamination kinetics from C-on-TiO_2 growth to C-on-C growth. We attempt to choose EUV doses that deposit no more than a (1-2) nm of C in order to measure the growth rate for the capping layer rather than the surface-independent C-on-C rate.

2.3 Post-exposure analysis

High-spatial-resolution metrology is required to resolve the variation in contamination across the roughly Gaussian dose distribution of our relatively small exposure spot. In the past, exposures of MLMs were characterized by 13.5-nm-reflectivity mapping with 100 μm step size at the Advanced Light Source of the Lawrence Berkeley National Laboratory. The one-standard-deviation relative uncertainty of these measurements was 0.08%, which was sufficient to detect absorption by sub-nanometer variations in deposited C thickness. However, due to the inherently resonant nature of MLMs, the reflectivity does not decrease monotonically with increasing C thickness on the mirror surface.[4] The exact relationship between C thickness and reflectivity depends on the details of the MLM design, the cap layer thickness, the thickness of any native adventitious C, and the density of the EUV-induced C deposits. If the added C thickness does not extend significantly into a maxima or minima of the standing wave created by the resonantly irradiated MLM, then the reflectivity decrease is quite linear with C thickness. The reflectivity data presented below were from exposures that resulted in C growth within this linear regime. Since our studies encompass different MLMs with different cap layers

exposed to different organic gases which may produce EUV-induced C depositions with different densities, we have moved away from using reflectometry alone for post-exposure characterization of our samples.

All measurements of C thickness reported here were performed using a commercial high-spatial-resolution x-ray photoelectron spectroscopy (XPS) surface probe tool with an analysis spot size of ≈ 250 µm. The C thickness at each location was determined using the spectra in the C 1s and Ti 2p energy regions produced by monochromatized Al Kα radiation (1486.6 eV). A spatial map of the deposited C like that shown in Fig. 2(a) was created for each exposure spot by taking measurements in 200 µm steps over a (2.0×2.0) mm grid. This analysis was performed *ex situ* which required transport of the exposed samples in air from the synchrotron beamline to the XPS system.

The spatial distribution of EUV dose for each exposure spot is known from ancillary measurements of the intensity profile and the recorded decay of the synchrotron current during the exposure. The dose distribution can therefore be mapped onto the spatial distribution of C thickness obtained from micro-XPS. Figure 2(a) shows an example of a false-color mapping of the measured C thickness distribution superimposed with contours of the EUV-dose distribution. By combining the data from all pixels in the image, a dose-response curve like that in Fig. 2(b) can be generated for each exposure spot. The linearity of these plots provides an important confirmation that there was not a significant change in contamination rate during the exposure due to either a non-linear intensity dependence or a transition from C-on-TiO_2 growth to C-on-C growth. No such departure from linearity was observed for the exposures reported here with intensities ranging from (1 to 8) mW/mm^2, doses from (40 to 200) J/mm^2 and resulting C thicknesses from (0.5 to 5) nm.

The absolute value of the estimated C thickness is proportional to the assumed electron scattering length, λ_e, which can vary by ±15% for different forms of deposited C.[12] An average of 3.2 nm was assumed here. This is the largest source of absolute uncertainty in our estimates of C thickness. For C thicknesses much less than 1 nm, however, uncertainties due to shot noise can dominate. The uncertainty in these cases can be as high as 20%.

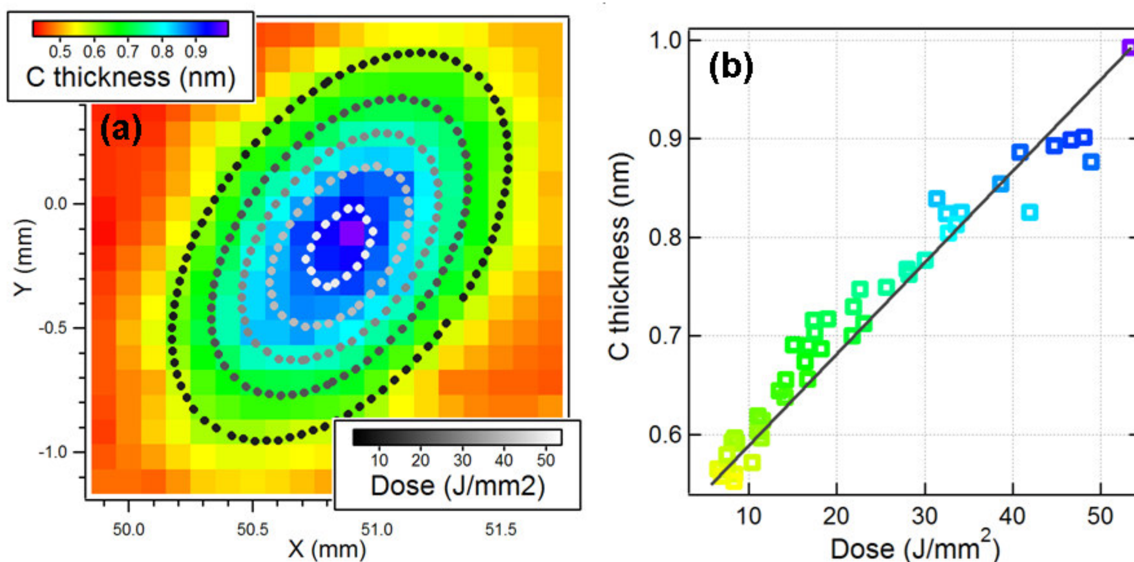

Figure 2. (a) False color image of typical carbon thickness distribution measured by XPS with superimposed contours of EUV dose distribution. (b) Data from (a) plotted as dose-response curve. The slope of the linear fit is the C-growth rate.

3. RESULTS

3.1 EUV-induced C contamination rates measured at NIST

Recent measurements of the carbon growth rates on TiO_2-capped tri-layer samples for benzene, isobutene (also called isobutylene or 2-methyl-1-propene), toluene and tert-butylbenzene over a large pressure range are shown in Fig. 3. These species were among the most prevalent detected in recent NIST measurements of EUV-induced outgassing from

several open source and proprietary resists. The composition of the outgas products was analyzed by gas-chromatography mass spectroscopy. Preliminary results analyzing the ambient vacuum of a pre-production tool using the same techniques indicated the presence of toluene and isobutene as well.[13]

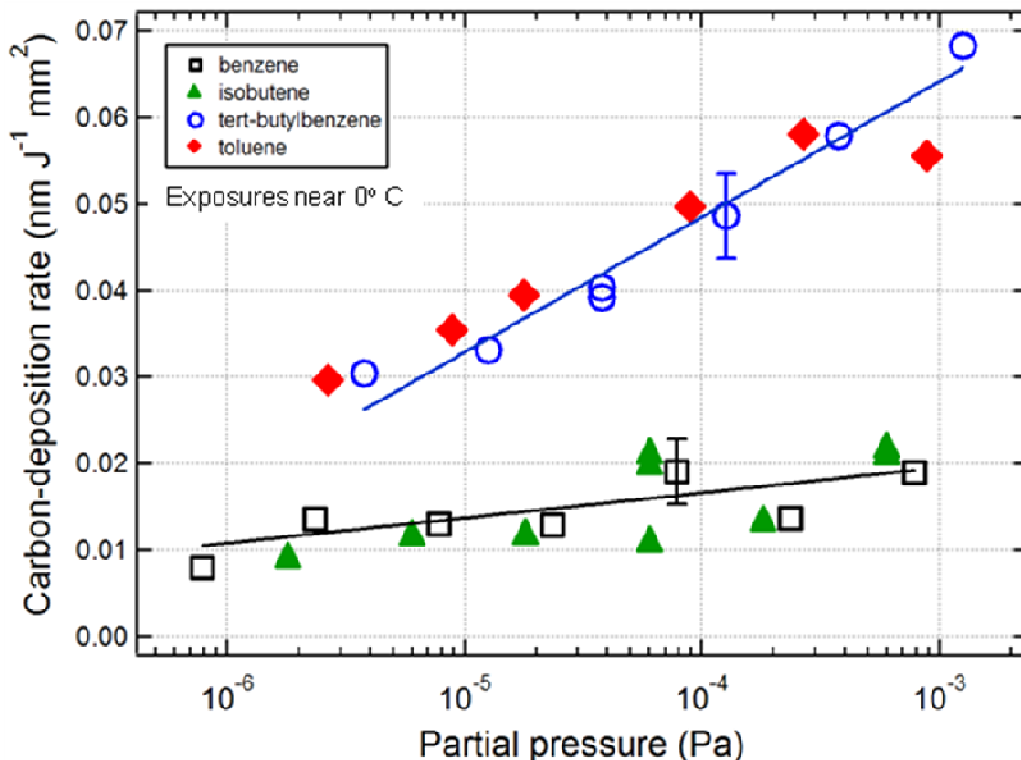

Figure 3. Carbon growth rates on TiO_2-capped trilayers samples for four anticipated contaminant gases. The average temperature during these exposures was near 0º C. Straight-line fits for benzene and tert-butylbenzene show logarithmic pressure dependence across 3 decades of pressure. The error bars reflect the relative uncertainty due primarily to counting statistics of XPS measurements. For the sub-nanometer C deposition produced by benzene and isobutene this was 20%. For the thicker deposits of toluene and tert-butlybenzene this was 10%. The uncertainty in absolute thickness common to all points is estimated to be ±15%.

The data in Fig. 3 are from exposures performed prior to the installation of temperature control of the sample. Due to cooling from a nearby cryogenic vacuum pump the samples likely began each exposure near room temperature and then were cooled to an equilibrium temperature within ±5º C of 0º C. While the photon and secondary-electron reaction rates are not expected to have a strong temperature dependence, the coverage of adsorbed molecules available for reaction likely does. So the absolute contamination rates reported here may be significantly different from those at room temperature (currently being measured), but this is not expected to change the observed logarithmic scaling with pressure.

Figures 4 and 5 show earlier measurements of carbon deposition on TiO_2-capped MLM samples exposed to EUV over a range of pressures of benzene, methyl methacrylate (MMA) and acetone. The data in Fig. 5 are from exposures performed in a different vacuum chamber with similar EUV irradiation conditions to those described in Sec. 2.1 above and with a stable sample temperature of (20º±5º) C. The contamination was characterized by measuring the relative reflectivity loss of the MLM after EUV exposures of 390 J/mm^2 which is 5-10 times larger than the doses used for the other data presented here. This resulted in an estimated (2 to 6) nm of C growth (assuming a reflectivity loss of 1% per nanometer of C) so that the underlying TiO_2 was covered by at least (1 to 2) nm of C through most of the exposures. Hence, these measurements show the same logarithmic pressure dependence is observed for this type of C-on-C growth as was found for the C-on-TiO_2 growth presented in Figs. 3 and 4.

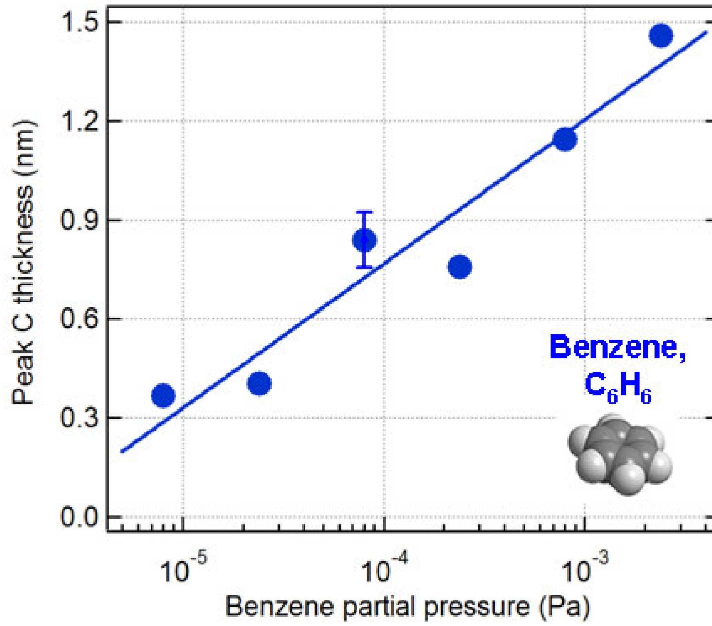

Figure 4. Estimated peak C thickness from 40 J/mm^2 EUV exposure of TiO_2-capped MLM in partial pressures of benzene. The straight-line fit shows the logarithmic scaling with pressure across nearly 3 decades. The error bar represents the ±10% uncertainty due primarily to counting statistics of XPS measurement. The uncertainty in absolute thickness common to all points is estimated to be ±15%.

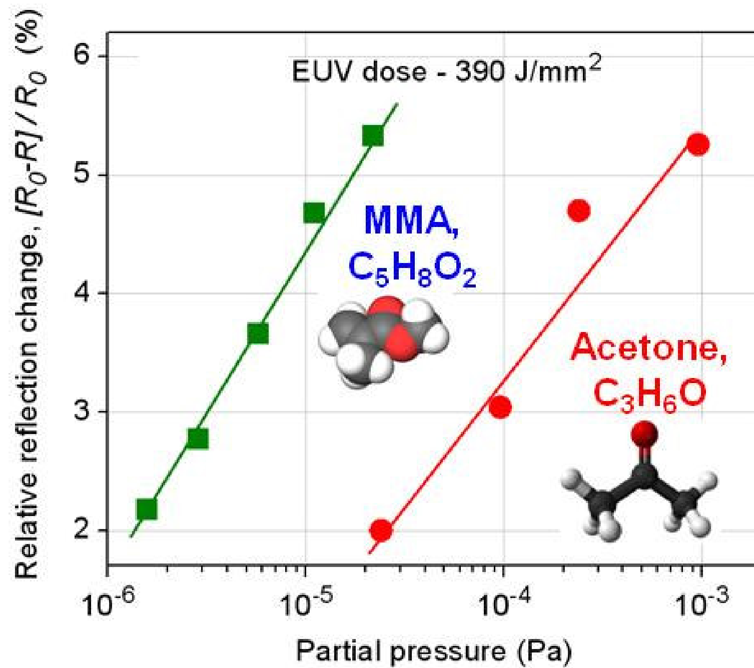

Figure 5. Peak reflectivity loss at 13.5 nm of TiO_2 MLM after high-dose EUV exposure to acetone and methyl methacrylate (MMA). Data suggest (2 to 6) nm of C was deposited so that the exposure was dominated by C-on-C growth. The straight-line fits suggest a logarithmic scaling of C deposition rates. Uncertainty of reflectivity measurements <0.1%.

3.2 Coverage measurements at Rutgers University

The unexpected logarithmic pressure scaling observed in the EUV-induced C-contamination rate measurements at NIST is consistent with independent work at Rutgers which measured the equilibrium coverage of molecules on a surface as a function of partial pressure. This work is described in detail in references 14 and 15. Briefly, the steady-state coverage of molecules on a clean $TiO_2(011)$ crystal in equilibrium with a fixed partial pressure of the gas is measured over a wide range of pressures. Temperature programmed desorption (TPD) was used to measure coverage in the low pressure regime of approximately (10^{-8} to $\approx 5\times10^{-7}$) Pa, and low-energy ion scattering (LEIS) was used for pressures from (10^{-7} to 10^{-4}) Pa.

Figure 6(a) shows the results of the LEIS measurements for MMA and benzene on clean $TiO_2(011)$ in the high pressure range, and Figs. 6(b,c) show the TPD results and for benzene and MMA on both clean and C-covered $TiO_2(011)$. (The C thickness was estimated to be 2 nm.) The coverage is reported in units of monolayers (ML) where 1 ML is the coverage sufficient to occupy every available surface site, typically $\approx 10^{19}$ molecules m^{-2}. The MMA coverage in Fig. 6(a) begins to saturate as it approaches 1 ML, but below this both MMA and benzene display the same logarithmic pressure dependence observed in the NIST EUV-contamination measurements. Figures 6(b,c) show that this scaling continues down to the lowest pressures measureable on both clean $TiO_2(011)$ and C-covered surfaces.

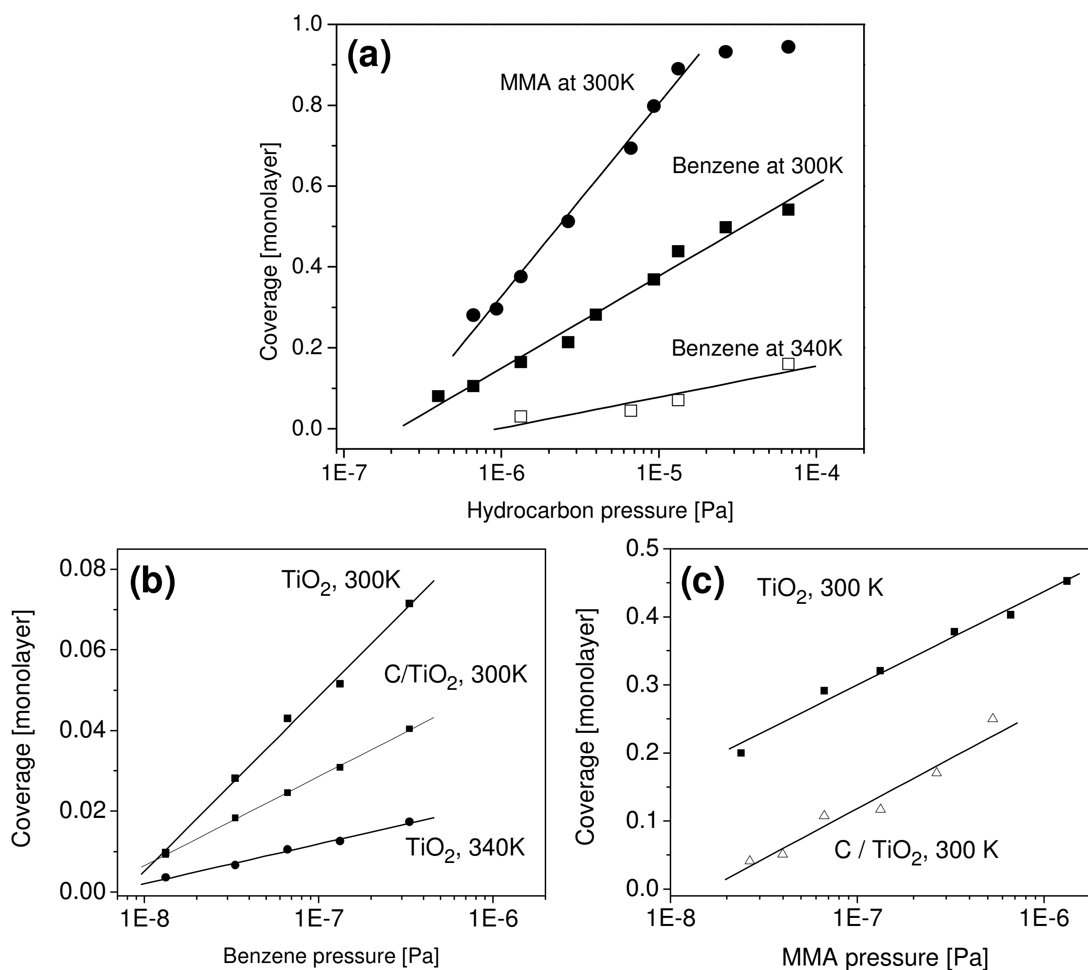

Figure 6. Coverage measurements performed at Rutgers University. (a) Steady state coverage at of benzene at 300 K and 340 K and methyl methacrylate (MMA) at 300 K on $TiO_2(011)$ in the high-pressure range obtained from low-energy ion scattering measurements. Steady state coverage of benzene (b) and MMA (c) on both clean and C-covered (≈2 nm) $TiO_2(011)$ in the low pressure range obtained by temperature programmed desorption (TPD) measurements. One monolayer is determined from ancillary TPD measurements as the saturation coverage in the first adsorbed layer. Pressures have not been corrected for ionization gauge sensitivity to different gases. (Data from Ref. 15.)

4. DISCUSSION

4.1 Correlation of coverage and contamination-rate measurements

Taken together, Figs. 3, 4 and 6 show that, in the pressure range studied, both the EUV-induced contamination rate and the steady-state coverage on TiO_2 surfaces scale logarithmically with pressure for a variety of gases and at different temperatures. The fact that the same behavior is seen on both 1.5-nm-thick amorphous layers of air-exposed TiO_2 and on UHV-cleaned-crystalline TiO_2(011) surfaces suggests that this is not a surface-specific phenomenon. Figures 5 and 6 strongly support this as well since the same logarithmic scaling of both contamination and coverage (respectively) is observed even for surfaces that are covered with 2 nm or more of carbon.

Further evidence that a logarithmic pressure scaling is more common than not with regard to MLM degradation can be found in the early (2003-2004) tests of the oxidation resistance of MLMs at NIST and Sandia National Laboratory.[16,17] In these studies Si-capped MLMs were exposed to both EUV irradiation and 1-keV electron-beam bombardment in the presence of elevated partial pressures of water vapor. The thickness of the oxide produced on the Si-terminated surface by equivalent exposures was observed to scale with the logarithm of water partial pressure over the range (10^{-6} to 10^{-4}) Pa for both e-beam and EUV irradiation. In 2006, Niibe, *et al* reported a similar scaling of reflectivity loss of Si-capped MLMs exposed to EUV radiation in partial pressures of water between (10^{-4} to 10^{-2}) Pa.[18] Together these data sets display a logarithmic pressure dependence of EUV-induced oxidation rate that spans more than 4 decades of pressure. Although these pressures are much higher than those used in the carbon-growth and coverage studies reported here, the desorption energy for water on most surfaces is much lower than that for large, organic molecules.[6] So despite the higher pressures, the range of equilibrium water coverages in the earlier oxidation-resistance studies may have been quite similar to the range of organic coverages in the experiments discussed here.

The fact that the pressure scaling is the same for both coverage and contamination rates of different gases on different surfaces and at different temperatures suggests that the C growth rate is proportional to coverage. This result is not unexpected since, to first order, one would expect the photon-induced reaction rate to be proportional to both the EUV intensity and the areal density of adsorbed molecules available to react. It is the underlying logarithmic variation of coverage with pressure that is the less intuitive departure from the usual Langmuir models which predict a non-linear pressure dependence only as the coverage approaches 1 ML, typically at higher pressures.

4.2 Possible origin of logarithmic pressure dependence

The most common approach to modeling the steady-state coverage of molecules adsorbed on the surface in equilibrium with the ambient partial pressure is to assume the Langmuir isotherm applies.[19] This model assumes that molecules adsorb intact and reversibly, that the desorption rate is constant, that there are no interactions between adsorbed molecules and that there is a finite density of identical adsorption sites that can each accommodate only one molecule at any given time. This results in a coverage, θ, of the form

$$\theta = \frac{a \cdot p \cdot \tau}{1 + a \cdot p \cdot \tau} \tag{1}$$

Here θ has units of ML, p is the pressure, a is a molecule-dependent constant and the residence time, τ, is the mean time a molecule spends on the surface before it is desorbed back into the gas phase. The residence time is related to the desorption energy of the molecule, E_d, by

$$\tau = \tau_0 \cdot \exp\left(\frac{E_d}{kT}\right) \tag{2}$$

where k is Boltzmann's constant, T is the temperature and τ_0 is a molecule-and-surface-dependent constant typically on the order of (10^{-12} to 10^{-14}) s. It is a key assumption of the Langmuir model that the residence time is constant and independent of coverage. Equation 1 predicts a linear dependence of coverage on pressure for $p \ll (a \cdot \tau)^{-1}$ (corresponding to $\theta \ll 0.5$ ML) and an approach towards saturation of 1 ML at higher pressures where competition for available sites limits further adsorption. Such site competition has been proposed as one possible explanation of the non-linear behavior observed in previous measurements of contamination rates over a relatively small range of pressures. This model, however, is much less consistent with the collection of measurements presented here which show that the non-linear trend spans multiple decades of pressure.

A commonly employed extension to the idealized Langmuir model is the so called Temkin isotherm.[19] Here it is assumed that repulsive interactions among adsorbed molecules will lead to a desorption energy that decreases linearly with coverage as $E_d=E_0 - \alpha\theta$. The other assumptions of the Langmuir model are retained. So this coverage-dependent desorption energy can be directly substituted into Eq. 2 to obtain a coverage-dependent residence time to be used in Eq. 1. This leads to a relationship between pressure and coverage of the form

$$\log\left(\frac{p}{p_0}\right) = \beta \cdot \theta + \log\left(\frac{\theta}{1-\theta}\right) \tag{3}$$

where β and p_0 are constants. This has no closed-form solution for θ as a function of p. If, however, the coverage is expected to be near 0.5 ML, the $\log[\theta/(1-\theta)]$ term is likely to be smaller and more slowly varying than the linear term so that the coverage can be approximated by

$$\theta \approx \frac{1}{\beta} \cdot \log\left(\frac{p}{p_0}\right), \quad \text{for } \theta \text{ near 0.5 ML} \tag{4}$$

In this form p_0 is seen to be equal to the x-axis-intercept of the straight-line fits to the data presented in Figs. 3-6. This approximate logarithmic pressure dependence is consistent with all the data presented here, even down to coverages as low as 0.01 ML. [See Figs. 6(b,c).] Although this is well below 0.5 ML cited for general validity of Eq. 4, the $\log[\theta/(1-\theta)]$ term in Eq. 3 is so slowly varying that for typical values of β (≈10-100) the scaling remains approximately logarithmic even at these low coverages. Additional measurements at Rutgers also demonstrate a clear linear decrease in desorption energy with coverage for MMA and benzene on clean and C-covered $TiO_2(011)$ surfaces, which is consistent with the underlying assumptions of the Temkin model.[15]

4.3 Low-pressure extrapolation and implications for optic lifetime estimates

The main goal of the this work is to develop a reliable testing method that will provide estimates of the contamination rates in the tool environment where partial pressures of organics are expected to be (10^{-10} to 10^{-8}) Pa from accelerated measurements performed with partial pressures in the range of (10^{-7} to 10^{-4}) Pa. While the Temkin model is one possible explanation of the observed logarithmic pressure dependence of coverage, direct application of this model to extrapolate contamination rates at very low pressures from higher-pressure measurements alone appears problematic at present.

All the C-contamination-rate, oxidation-rate and coverage data presented here suggest a simple $\log(p)$ scaling over a wide range of pressures. While this provides very strong evidence that a model incorporating molecule-molecule interactions, such as Temkin, should be considered, a logarithmic variation such as Eq. 4 cannot be extrapolated to low pressures because it diverges below p_0. In fact, the approximation leading to Eq. 4 will become invalid at pressure much below $\approx 10\times p_0$ at which point Eq. 3 predicts a transition to linear scaling of coverage with pressure. Unfortunately there is no evidence of this changeover in any of the data, making it difficult to predict how the measurements should be extrapolated to lower pressures. What is clear from the logarithmic scaling over such a wide range of pressures is that linear extrapolation of high-pressure data over several orders of magnitude would likely underestimate the coverage or contamination rate by multiple orders of magnitude at the lower pressures.

Although understanding the scaling behavior is critical, the influence of ambient water vapor must also be taken into account. The NIST exposures are performed in a UHV chamber with a base partial pressure of water near 10^{-8} Pa, and the Rutgers coverage measurements are carried out at even lower base pressures. These conditions are necessary to understand the fundamental processes of C-deposition and molecular coverage. In the tool environment, however, the partial pressures of the organic species will always be significantly less than the partial pressure of water vapor which is anticipated to be on the order of 10^{-5} Pa. Preliminary tests at NIST and recent results from The University of Hyogo, Japan[20] of EUV exposures in admixtures of organic species and water vapor show a significant reduction in the contamination rates compared to exposures in the organic species alone. This data along with previous work at NIST[21] also show that the addition of water vapor to EUV exposures can sometimes produce highly non-intuitive intensity and dose dependencies.

5. SUMMARY

One of the goals of the EUV-optics contamination program at NIST is to estimate the long-term risk to optics posed by exposure to EUV in very low partial pressures of organic contaminants expected in the tool. This requires an understanding of how the contamination rates measured at higher partial pressures can be scaled down to these lower pressures. Here, we present a large body of evidence suggesting that suggests this scaling is substantially slower than a simple linear dependence on pressure. Instead, EUV exposures at NIST of amorphous-TiO_2-capped surfaces in the presence of methyl methacrylate (MMA), acetone, benzene, isobutene, toluene and tert-butylbenzene all result in carbon-contamination rates that appear to scale with the logarithm of partial pressure over the range (10^{-6} to 10^{-4}) Pa. These results are consistent with independent measurements at Rutgers University which show that for MMA and benzene vapors in equilibrium with both clean and carbon-covered $TiO_2(011)$ surfaces the steady-state coverage of adsorbed molecules scales logarithmically with partial pressure over an even wider range of (10^{-8} to 10^{-4}) Pa. Even data from previous studies of Si-capped MLMs exposed to EUV in the presence of water vapor suggest a logarithmic dependence of the degree of Si oxidation on the partial pressure of water.

One possible explanation of this behavior is the Temkin isotherm which assumes that the desorption energy decreases linearly with coverage due to repulsion between adsorbed molecules. This model predicts an approximate logarithmic pressure dependence of coverage over a limited range of coverage, below which a linear scaling is expected. However, since this transition from simple $\log(p)$ scaling has not been observed in any of the data, straightforward extrapolation of the existing contamination-rate measurements with this model is not possible. There may not be a single "universal" scaling law that can accurately predict the coverage or contamination rate over the 6 orders of magnitude that span the pressures where most testing is performed [(10^{-6} to 10^{-4}) Pa] down to the partial pressures expected in the tool environment [(10^{-10} to 10^{-8}) Pa]. All the data presented here suggest that a logarithmic pressure scaling is most appropriate for pressures down to 10^{-8} Pa, but extrapolation beyond this requires measurements at lower pressures that include the potential effects of an admixture of water vapor.

To address these issues, the range of contaminant partial pressures used during exposures at NIST is being extended to lower levels and exposures are performed with and without an admixture of 10^{-5} Pa water vapor for each organic species tested. Based on the NIST and Rutgers data presented here, we feel that these measurement protocols are required to avoid dramatic underestimation of the contamination rates in the tool. If linear extrapolation from a few high-pressure measurements were used instead, it seems likely that the tool contamination rates could be underestimated by multiple orders of magnitude.

ACKNOWLEDGEMENTS

We would like to thank James Clarke of Intel for very helpful discussions. This work supported in part by Intel Corporation.

REFERENCES

[1] Silverman, P.J., "Extreme ultraviolet lithography: overview and development status", J. Microlith., Microfab., and Microsys. 4(1), 01100 (2005)
[2] Seisyan, R.P., "Extreme ultraviolet nanolithography for ULSI: A review", Techn. Phys. 50(5), 535-545 (2005)
[3] See for example: H. Dannetun, I. Lundström, L. -G. Petersson, "The relative ionization gauge sensitivity of some unsaturated hydrocarbons", Applied Surface Science, Volume 29, Issue 3, November 1987, Pages 361-366; Sensitivity factors for gases used here: benzene, 5.9; toluene, 6.8; isobutene, 4.6; acetone, 3.6; methyl methacrylate, 5.3 (estimated); tert-butylbenzene, 9.5 (estimated)
[4] S. B. Hill, *et al*, "Accelerated lifetime metrology of EUV multilayer mirrors in hydrocarbon environments," Proc. SPIE 6921, 42 (2008)
[5] S. Matsunari, *et al*, "Carbon deposition on multi-layer mirrors by extreme ultra violet ray irradiation," Proc. SPIE 6517, 107 (2007)
[6] T. E. Madey, N. S. Faradzhev, B. V. Yakshinskiy, N. V. Edwards, "Surface phenomena related to mirror degradation in extreme ultraviolet (EUV) lithography," Applied Surface Science **253**, p. 1691 (2006)

[7] B. V. Yakshinskiy, R. Wasielewski, E. Loginova, and T. E. Madey, "Carbon accumulation and mitigation processes, and secondary electron yields of ruthenium surfaces," Proc. SPIE 6517, 65172Z (2007)
[8] Samples fabricated by Sergiy Yulin at The Fraunhofer Institut Angewandte Optik und Feinmechanik to be 1.5 nm TiO2 on 4.0 nm Si on 2.9 nm Mo on a Si substrate. Uncertainty of all thicknesses is ±0.1 nm.
[9] C. Mbanaso, G. Denbeaux, K. Dean, R. Brainard, S. Kruger, and E. Hassanein, "Investigation of sensitivity of extreme ultraviolet resists to out-of-band radiation," Proc. SPIE 6921, 69213L (2008)
[10] Database of optical constants in the EUV at http://henke.lbl.gov/optical_constants, maintained by the Center for X-ray Optics, Lawrence Berkeley National Laboratory (http://www-cxro.lbl.gov)
[11] B. V. Yakshinskiy, M. N. Hedhili, S. Zalkind, M. Chandhok, and T. E. Madey, "Radiation-induced defect formation and reactivity of model TiO2 capping layers with MMA: a comparison with Ru," Proc. SPIE 6921, 14 (2008)
[12] S. Tanuma, C. J. Powell, D. R. Penn, "Calculations of electron inelastic mean free paths. V. Data for 14 organic compounds over the," Surf. Interf. Anal. 21, 165 (1993)
[13] C. Tarrio, R. E. Vest, S. E. Grantham, T. Lucatorto, R. Caudillo, "Tracking down sources of carbon contamination in EUVL exposure tools," Proc. of SPIE 7271, 38 (2009)
[14] S. Zalkind, B. V. Yakshinskiy, T. E. Madey, "Interaction of benzene with TiO2 surfaces: Relevance to contamination of extreme ultraviolet lithography mirror capping layers," J. Vac. Sci. Technol. B **26**, p. 2241 (2008)
[15] B. V. Yakshinskiy, S. Zalkind, R. A. Bartynski, R. Caudillo, T. E. Madey, "Carbon film growth on model electron-irradiated MLM cap layer: interaction of benzene and MMA vapor with TiO_2 surfaces," Proc. SPIE 7271, 36 (2009)
[16] M. E. Malinowski, C. A. Steinhaus, D. E. Meeker, W. M. Clift, L. E. Klebanoff, S. Bajt, "Relation between electron and photon caused oxidation in EUVL optics," Proc. SPIE 5040, 477-486 (2003)
[17] W. M. Clift, *et al*, "Scaling studies of capping layer oxidation by water exposure with EUV radiation and electrons," Emerging Lithographic Technologies VIII, ed. R. Scott Mackay, Proceedings of SPIE 5374, 0277-786X (2004)
[18] M. Niibe, *et al*, "New contamination experimental equipment in the NewSUBARU and evaluation of Si-capped multilayer mirrors using it," Proc. SPIE 6151, 34 (2006)
[19] R. I. Masel, Principles of Adsorption and Reaction on Solid Surfaces, Wiley-Interscience, p. 235 (1996)
[20] M. Niibe, K. Koida, "Experiment of contamination generation by EUV irradiation with the use of high-mass hydrocarbon gas," 2008 International Symposium on Extreme Ultraviolet Lithography, Lake Tahoe, NV (2008)
[21] S. B. Hill, I. Ermanoski, C. Tarrio, T. B. Lucatorto, T. E. Madey, S. Bajt, M. Fang, M. Chandhok, "Critical parameters influencing the EUV-induced damage of Ru-capped multilayer mirrors," Proc. SPIE 6517, 15 (2007)